DYNAMIC VISCOELASTIC INCREMENTAL-LAYERWISE FINITE ELEMENT METHOD FOR MULTILAYERED STRUCTURE ANALYSIS BASED ON THE RELAXATION APPROACH

M. Malakouti *

Department of Civil Engineering
Persian Gulf University
Bushehr, Iran

M. Ameri

Mahmoud Ameri, Professor and Director of Center of Excellence for PMS
Transportation and Safety
Iran University of Science & Technology

P. Malekzadeh

Department of Mechanical Engineering
Persian Gulf University
Bushehr, Iran

ABSTRACT

This paper presents an axisymmetric layerwise finite element formulation for dynamic analysis of laminated structures with embedded viscoelastic material whose constitutive behavior is represented by the Prony-generalized Maxwell series. To account the time dependence of the constitutive relations of linear viscoelastic materials, the incremental formulation in the temporal domain is used. Layerwise finite element has been shown to provide an efficient and accurate tool for the simulation of laminated structure. Most of the previous work on numerical simulation of laminated structures has been limited to elastic material behavior. Thus, the current work focuses on layerwise finite element analysis of laminated structures with embedded viscoelastic material. A computer code based on the presented formulation has been developed to provide the numerical results. The present approach is verified by studying its convergence behavior and comparing the numerical results with those obtained using the ABAQUS software. Finally, and as an application of the presented formulation, the effects of load duration on the dynamic structural responses of multilayered pavements are studied.

Keywords: Layerwise finite element, Viscoelastic behavior, Incremental formulation, Dynamic response, Prony series.

1. INTRODUCTION

Studying the laminated structures with embedded viscoelastic material has attracted many researchers [1-5].The significant use of viscoelastic materials in engineering structures needs understanding the behavior of time-dependent mechanical stresses and deformations that can cause failure of such structures. The principle problem in representing a mathematical model for the mechanical behavior of these materials is that their responses depend on their complete history of stress and strain tensor components and consequently, the solutions of these types of problems become more complicated than those of the related elastic ones. For this reason, some researchers applied the integral transform methods (*e.g.*, Fourier and Laplace transforms) to the constitutive equation of the viscoelastic material first, and then employed the correspondence principle (see for example Refs. [6,7]). However, there are two main challenges in solving the viscoelastic multilayer response by using the correspondence principle. The first challenge is the difficulty of obtaining the associated elastic solution for a multilayered structure, and the other one is associated with the inverse transform that is more difficult to invert the transform analytically. Since most of the existing analytical solutions require the retaining of the complete history of the stresses and strains in the memory of a digital computer for real and complex problems, these methods cannot deal with such problems [8,9]. To overcome this shortcoming, a number of theories based on the incremental constitutive relations for the analysis of linear viscoelastic problems have been proposed in the past. For example, the incremental constitutive relations in conjunction with the finite element method have been employed in Refs. [8-14].

Different types of mathematical models for the behavior of viscoelastic materials are usually obtained by

* Corresponding author (malakooti@pgu.ac.ir)

DOI : 10.1017/jmech.2014.42
Copyright © 2014 The Society of Theoretical and Applied Mechanics, R.O.C.
https://doi.org/10.1017/jmech.2014.42 Published online by Cambridge University Press

means of different arrangements of spring (s) and dashpot (s); for example, generalized models (Prony series models) such as the generalized Kelvin-Voigt model consisting of a spring and *N* Voigt elements connected in series [8,12-14] and the generalized Maxwell model consisting of a spring and *M* Maxwell elements connected in parallel [9, 15-19], sigmoidal models [20], parabolic models [21,22], power law model [23], *etc*. In the present paper, a Prony-generalized Maxwell series is adopted, which has been employed by the researchers for the modeling of asphalt pavement behavior [15-17].

A displacement based layerwise finite element method (LW-FEM) has been introduced by Reddy [24] to accurately determine transverse shear and normal stress distributions of laminated composites based on the three-dimensional elasticity theory. This method was increasingly used by others as in the original form proposed by Reddy or in its extended forms in the solution of engineering problems, such as laminated structures [25-31] during recent years. The layerwise theory is a refined theory that can take into account the thickness effects with minimum computational cost [29-31]. Since the layerwise theories assume a separate displacement field expansions within each subdivision, it provides a kinematically correct representation of the strain field in discrete layers [24,31]. In addition, because the shear strains are discontinuous, this leaves the possibility of the continuous transverse stresses between adjacent layers in the layerwise theory. For the two-dimensional problems, the approach actually shrinks the modeling to a combined from two one-dimensional analysis, which considerably reduces the number of manipulations, and the complexity in the formulation of the 2D finite element method. Implementing such methodology is not possible in powerful software like ABAQUS, which are developed based on the conventional FEM.

In this work, in order to carry out the dynamic analysis a simple and efficient algorithm based on the viscoelastic incremental LW-FEM for the axisymmetric analysis of multilayer viscoelastic structure and in particular, multilayer pavements is presented. In this algorithm, stresses are written as hereditary integrals with the relaxation modulus represented by a Prony-Maxwell series, whereas the dynamic equilibrium equations are integrated by the Newmark's method. Details of the LW-FE formulation, verification and an asphalt concrete pavement simulation example are presented and structural parameters typically used in pavement analysis are evaluated.

2. VISCOELASTIC MATERIALS

With the linearity assumption, the constitutive equation, between the components of the stress tensor σ_{ij} and the components of the strain tensor ε_{kl}, can be expressed in the time domain by the hereditary Volterra's integral equation. Using the Boltzmann [32] superposition principle, the stress-strain relationship of a viscoelastic material can be expressed in tensor notation as

$$\sigma_{ij}(t) = \int_0^t C_{ijkl}(t-\tau)\frac{\partial \varepsilon_{kl}(\tau)}{\partial \tau}\, d\tau \tag{1}$$

where σ_{ij} and ε_{kl} are the components of the stress and strain tensors, respectively; C_{ijkl} is the fourth order tensor of relaxation modulus relating stress to mechanical strain; τ is the time variable and t is the time since loading.

In order to evaluate the hereditary integral in Eq. (1), it is necessary to express the relaxation modulus as a mathematical function. In the present paper, a Prony-generalized Maxwell series is used for this purpose:

$$C_{ijkl}(t) = \left[C_{ijkl}^{(0)} + \sum_{m=1}^{M} C_{ijkl}^{(m)} e^{-\frac{t}{\rho_{ijkl}^{(m)}}} \right] H(t) \tag{2}$$

where $C_{ijkl}^{(0)}$ and $C_{ijkl}^{(m)}$ are equilibrium modulus and relaxation strength, respectively; $\rho_{ijkl}^{(m)}$ is the relaxation time and $H(t)$ is the unit step function.

From Eq. (1) it is obvious that the response is a function of not only the current input but also of the past input history. The constitutive relations represented by Eq. (1) can be expressed into an incremental form in order to be used with a layerwise finite element method. The use of incremental form has the advantage of eliminating the memory possessing problem because it does not need to solve a set of differential equations simultaneously. In this study, the numerical algorithm proposed by Zocher *et al*. [9] is adopted. This approach is based on a time discretization of the relaxation function according to Prony series represented in Eq. (2). According to this algorithm, the constitutive relation in terms of the relaxation function is transformed from integral form into an incremental algebraic form by a Prony series representation prior to development of the layerwise finite element formulation. In the following, the main formulations and principles of this algorithm are briefly described.

In this algorithm, the time corresponding to the next step $n + 1$ is obtained from the current time t_n, such that $\Delta t_n = t_{n+1} - t_n$.

where Δt_n is a time increment between the two steps. Assuming that stresses are known at time t_n, the objective is to compute the stress increment $\Delta\sigma_{ij}$ that occurs during the increment Δt_n. Incremental constitutive relations in each time interval Δt_n can be written as [9],

$$\Delta\sigma_{ij} = \bar{C}_{ijkl} \,.\, \Delta\varepsilon_{kl} + \Delta\sigma_{ij}^{R} \tag{3}$$

where $\Delta\varepsilon_{kl}$ and $\Delta\sigma_{ij}$ are the increments of strain and stress tensor components, respectively, and $\bar{C}_{ijkl}$ is a fourth-order tensor which can be interpreted as a viscoelastic relaxation tensor,

$$\bar{C}_{ijkl} = C_{ijkl}^{(0)} + \frac{1}{\Delta t_n}\sum_{m}^{M} \rho_{ijkl}^{(m)} C_{ijkl}^{(m)} \left[1 - e^{-\frac{\Delta t_n}{\rho_{ijkl}^{(m)}}} \right] \tag{4}$$

From Eq. (4) it is obvious that $\bar{C}_{ijkl}$ depends not only on the material properties but also on the time in-

https://doi.org/10.1017/jmech.2014.42 Published online by Cambridge University Press

crement Δt_n. The second term in the r.h.s. of Eq. (3) represents the viscous or hereditary part of the stress increment can be written as,

$$\Delta\sigma_{ij}^{R} = -\sum_{m}^{M}\left[1-e^{-\frac{\Delta t_n}{\rho_{ijkl}^{(m)}}}\right]S_{ijkl}^{(m)}(t_n) \tag{5}$$

where the parameters $S_{ijkl}^{(m)}$ can be computed by the following recursive expression,

$$S_{ijkl}^{(m)}(t_n) = e^{-\frac{\Delta t_n}{\rho_{ijkl}^{(m)}}}S_{ijkl}^{m}(t_{n-1}) + \rho_{ijkl}^{(m)}C_{ijkl}^{(m)}\dot{\varepsilon}_{kl}(t_{n-1})\left(1-e^{-\frac{\Delta t_n}{\rho_{ijkl}^{(m)}}}\right) \tag{6}$$

where $\dot{\varepsilon}_{kl}(t_{n-1})$ is constant representing the time rate of change over the interval from time step t_{n-1} to t_n. When using small time increments, it is possible to assume a constant strain rate variation during the interval. Thus

$$\dot{\varepsilon}_{kl} = \frac{\partial\varepsilon_{kl}}{\partial t} \cong \frac{\Delta\varepsilon_{kl}}{\Delta t} \tag{7}$$

For a complete solution of the algorithm regarding the incrementalization method, refer to Zocher *et al.* [9]. The incremental constitutive law represented by Eq. (3) can be introduced in a layerwise finite element discretization in order to obtain solutions to complex viscoelastic problems.

3. AXISYMMETRIC LAYERWISE FINITE ELEMENT FORMULATION

Usually an axisymmetric computational domain is selected to numerically simulate multilayered structures such as the multilayer pavements under single tire loading [13,33-35]. Using the axisymmetric modeling could simulate circular loading and also do not require excessive computational time. A typical axisymmetric computational domain for the multilayer pavement modeling is shown in Fig. 1. As shown in this figure, the bottom surface of the subgrade is assumed to be fixed, which means that nodes at the bottom of the subgrade cannot move horizontally or vertically. Also, the boundary nodes along the vertical pavement surface are horizontally constrained, but are free to move in the vertical direction.

Based on the two-dimensional theory of elasticity, the linearized axisymmetric strain-displacement relations are as follows [36],

$$\{\varepsilon_{ij}\}^T = [\varepsilon_{rr}\ \ \varepsilon_{zz}\ \ \varepsilon_{\theta\theta}\ \ \gamma_{rz}] = \left[\frac{\partial u}{\partial r}\ \ \frac{\partial w}{\partial z}\ \ \frac{u}{r}\ \ \frac{\partial u}{\partial z}+\frac{\partial w}{\partial r}\right] \tag{8}$$

where ε_{ii} ($i = r, z, \theta$) and γ_{rz} are the normal and shear components of the strain tensor at an arbitrary material points of the domain, respectively.

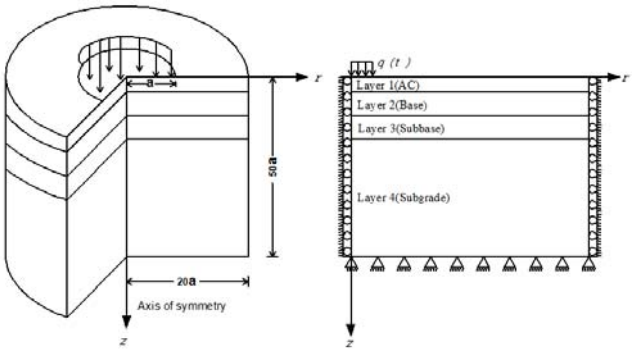


Fig. 1 Multilayer pavement section, loading and boundary conditions.

Based on the layerwise theory, the laminated structure in the thickness direction is subdivided into a series of N_{ML} mathematical layers. In each mathematical layer, the displacement components in the thickness direction are approximated in a similar manner as the one-dimensional finite elements method. In this direction, one has N_z nodes, which relates to the number of mathematical layers N_{ML} and the node per layer N_{PL} according to $N_z = (N_{PL}-1)\,N_{ML} + 1$. The layerwise concept is very general in the way that the number of subdivisions through the thickness can be greater than, equal to, or less than the number of material or physical layers through the thickness. Independent shape functions are defined in the plate thickness and the radial directions. Any desired degree of displacement variation through the thickness is easily obtained by either adding more 1-D mathematical layers or using the higher-order Lagrangian interpolation polynomials through the plate thickness. In this analysis, the linear global shape functions $\psi_j(z)$ (with j = 1, 2, 3, …, N_z) and $\varphi_i(r)$ (with i = 1, 2, 3, …, N_r) are used along the thickness and radial directions, respectively. For the case of the two nodes per mathematical layers in the thickness direction and r-direction elements, the global interpolation functions become, respectively,

$$\psi_j(z) = \begin{cases} 0 & z \le z_{j-1},\ z_{j+1} \le z \\ \dfrac{z-z_{j-1}}{z_j - z_{j-1}} & z_{j-1} \le z \le z_j \\ \dfrac{z_{j+1}-z}{z_{j+1}-z_j} & z_j \le z \le z_{j+1} \end{cases}, \tag{9a}$$

$$\phi_i(r) = \begin{cases} 0 & r \le r_{i-1},\ r_{i+1} \le r \\ \dfrac{r-r_{i-1}}{r_i - r_{i-1}} & r_{i-1} \le r \le r_i \\ \dfrac{r_{i+1}-r}{r_{i+1}-r_i} & r_i \le r \le r_{i+1} \end{cases} \tag{9b}$$

where i = 1, 2, 3, …, N_r and j = 1, 2, 3, …, N_z; and r_i and z_j are the r and z-coordinate of the global nodes i and j, respectively.

https://doi.org/10.1017/jmech.2014.42 Published online by Cambridge University Press

In an incremental displacement-based formulation, the incremental displacement components at any material point of the pavement can be expressed as,

$$\Delta u_r = u_r(r, z, t+\Delta t) - u_r(r, z, t) = \sum_{i=1}^{N_r}\sum_{j=1}^{N_z} \Delta U_{ij}(t)\phi_i(r)\psi_j(z) = \Delta U_{ij}(t)\phi_i(r)\psi_j(z) \tag{10a}$$

$$\Delta u_z = u_z(r, z, t+\Delta t) - u_z(r, z, t) = \sum_{i=1}^{N_r}\sum_{j=1}^{N_z} \Delta W_{ij}(t)\phi_i(r)\psi_j(z) = \Delta W_{ij}(t)\phi_i(r)\psi_j(z) \tag{10b}$$

where Δu_r and Δu_z are the incremental displacement components of an arbitrary material point in the r and z-direction, respectively; $\Delta U_{ij}(t)$ and $\Delta W_{ij}(t)$ are the incremental displacement components of the nodal point (r_i, z_j) along the r and z-direction, respectively; also, as obvious from Eqs. 10(a), 10(b), for brevity purpose the indicial summation notation is used.

Based on the constitutive relations Eq. (3), the incremental constitutive relations at an arbitrary material point of an axisymmetric viscoelastic layer become,

$$\begin{Bmatrix}\Delta\sigma_{rr}\\ \Delta\sigma_{zz}\\ \Delta\sigma_{\theta\theta}\\ \Delta\sigma_{rz}\end{Bmatrix} = \begin{bmatrix}\bar{C}_{11} & \bar{C}_{12} & \bar{C}_{13} & 0\\ \bar{C}_{12} & \bar{C}_{22} & \bar{C}_{23} & 0\\ \bar{C}_{13} & \bar{C}_{23} & \bar{C}_{33} & 0\\ 0 & 0 & 0 & \bar{C}_{44}\end{bmatrix}\begin{Bmatrix}\Delta\varepsilon_{rr}\\ \Delta\varepsilon_{zz}\\ \Delta\varepsilon_{\theta\theta}\\ \Delta\gamma_{rz}\end{Bmatrix} + \begin{Bmatrix}\Delta\sigma^R_{rr}\\ \Delta\sigma^R_{zz}\\ \Delta\sigma^R_{\theta\theta}\\ \Delta\sigma^R_{rz}\end{Bmatrix} = [\bar{C}]\{\Delta\varepsilon_{ij}\} + \{\Delta\sigma^R_{ij}\} \tag{11}$$

where $\Delta\sigma_{ii}$ ($i = r$, z, θ) and $\Delta\sigma_{rz}$ are the incremental normal and shear components of the stress tensor, respectively; $[\bar{C}]$ is the material stiffness matrix of the viscoelastic material in the principle coordinates of the layer. Substituting the displacement components from Eqs. 10(a), 10(b) into Eq. (8), the results become,

$$\Delta\varepsilon_{rr} = \Delta U_{ij}\,\psi_j\frac{d\phi_i}{dr}, \tag{12a}$$

$$\Delta\varepsilon_{zz} = \Delta W_{ij}\,\phi_i\frac{d\psi_j}{dz}, \tag{12b}$$

$$\Delta\varepsilon_{\theta\theta} = \Delta U_{ij}\left(\frac{\phi_i\psi_j}{r}\right), \tag{12c}$$

$$\Delta\gamma_{rz} = \Delta U_{ij}\phi_i\frac{d\psi_j}{dz} + \Delta W_{ij}\,\psi_j\frac{d\phi_i}{dr} \tag{12d}$$

The incremental equations of motion during the time step Δt can be derived using the principle of virtual work as follows,

$$\begin{aligned}&\int_{R_i}^{R_o}\int_0^h\left[\Delta\sigma_{rr}\delta(\Delta\varepsilon_{rr}) + \Delta\sigma_{zz}\delta(\Delta\varepsilon_{zz}) + \Delta\sigma_{\theta\theta}\delta(\Delta\varepsilon_{\theta\theta}) + \Delta\sigma_{rz}\delta(\Delta\gamma_{rz})\right] r\,dz\,dr\\ &-\int_{R_i}^{R_o}\Delta q_z(r,t)\phi_i(r)\delta_{jN_z}\delta(\Delta W_{ij})\,r\,dr\\ &-\int_0^h\Delta q_r(z,t)\psi_j(z)\delta_{i1}\delta(\Delta U_{ij})\,r\,dz\\ &+\int_{R_i}^{R_o}\int_0^h\rho\left[\Delta\ddot{U}\,\delta(\Delta U_{ij}) + \Delta\ddot{W}\,\delta(\Delta W_{ij})\right] r\,dz\,dr = 0\end{aligned} \tag{13}$$

where the symbol δ is the variational operator and dot over a displacement components means its derivative with respect to time; $\Delta q_z(r, t)$ and $\Delta q_r(z, t)$ are the incremental external transverse and radial load, respectively; ρ, R_i, R_o and h are the mass density, the inner radius, the outer radius and the total thickness of the laminated domain, respectively; also, δ_{ij} is the Kronecker delta.

Using Eqs. (9) ~ (12), the discretized equations of motion can be extracted from Eq. (13) as,

$$\begin{bmatrix}[M_{uu}] & [0]\\ [0] & [M_{ww}]\end{bmatrix}\begin{Bmatrix}\{\Delta\ddot{U}\}\\ \{\Delta\ddot{W}\}\end{Bmatrix} + \begin{bmatrix}[K_{uu}] & [K_{uw}]\\ [K_{wu}] & [K_{ww}]\end{bmatrix}\begin{Bmatrix}\{\Delta U\}\\ \{\Delta W\}\end{Bmatrix} = \begin{Bmatrix}\{\Delta f_r\}\\ \{\Delta f_z\}\end{Bmatrix} - \begin{Bmatrix}\{\Delta f_r^R\}\\ \{\Delta f_z^R\}\end{Bmatrix} \tag{14}$$

where $\begin{Bmatrix}\{\Delta f_r\}\\ \{\Delta f_z\}\end{Bmatrix}$ and $\begin{Bmatrix}\{\Delta f_r^R\}\\ \{\Delta f_z^R\}\end{Bmatrix}$ are the external load vector increment and load vector increment corresponding to change of stresses during the time step. The elements of the stiffness matrices $[K_{ij}]$ (i, $j = u$, w), the mass matrices $[M_{ij}]$ (i, $j = u$, w) and the load vector increments $\begin{Bmatrix}\{\Delta f_r\}\\ \{\Delta f_z\}\end{Bmatrix}$ and $\begin{Bmatrix}\{\Delta f_r^R\}\\ \{\Delta f_z^R\}\end{Bmatrix}$ are presented in appendix A.

Equation (14) can be expressed into the following general form

$$[M]\{\Delta\ddot{D}\} + [K]\{\Delta D\} = \{\Delta F^{ext}\} - \{\Delta F^{vis}\} \tag{15}$$

where $[M] = \begin{bmatrix}[M_{uu}] & [0]\\ [0] & [M_{ww}]\end{bmatrix}$, $\{\Delta\ddot{D}\} = \begin{Bmatrix}\{\Delta\ddot{U}\}\\ \{\Delta\ddot{W}\}\end{Bmatrix}$,

$[K] = \begin{bmatrix}[K_{uu}] & [K_{uw}]\\ [K_{wu}] & [K_{ww}]\end{bmatrix}$, $\{\Delta D\} = \begin{Bmatrix}\{\Delta U\}\\ \{\Delta W\}\end{Bmatrix}$,

$\{\Delta F^{ext}\} = \begin{Bmatrix}\{\Delta f_r\}\\ \{\Delta f_z\}\end{Bmatrix}$ and $\{\Delta F^{vis}\} = \begin{Bmatrix}\{\Delta f_r^R\}\\ \{\Delta f_z^R\}\end{Bmatrix}$

For the problems where the loading is applied quasi-statically, the inertia forces can be neglected, which simplify the integration algorithm. In this case, Eq. (15) reduces to

$$[K]\{\Delta D\} = \{\Delta F^{ext}\} - \{\Delta F^{vis}\} \tag{16}$$

https://doi.org/10.1017/jmech.2014.42 Published online by Cambridge University Press

4. DYNAMIC ANALYSIS

In this study, the dynamic equilibrium Eq. (15) is integrated by the Newmark's algorithm with constant average acceleration [36]. In this method the nodal displacements and velocities are approximated by the expressions

$$\{D\}_{t_{n+1}} = \{D\}_{t_n} + \frac{1}{2}\left(\{\dot{D}\}_{t_{n+1}} + \{\dot{D}\}_{t_n}\right)\Delta t_n \,, \tag{17a}$$

$$\{\dot{D}\}_{t_{n+1}} = \{\dot{D}\}_{t_n} + \frac{1}{2}\left(\{\ddot{D}\}_{t_{n+1}} + \{\ddot{D}\}_{t_n}\right)\Delta t_n \tag{17b}$$

Thus, the new displacements, velocities, and accelerations can be written as

$$\{D\}_{t_{n+1}} = \{D\}_{t_n} + \{\Delta D\} \,, \tag{18a}$$

$$\{\dot{D}\}_{t_{n+1}} = \frac{2}{\Delta t_n}\{\Delta D\} - \{\dot{D}\}_{t_n} \,, \tag{18b}$$

$$\{\ddot{D}\}_{t_{n+1}} = \frac{4}{\Delta t_n^2}\{\Delta D\} - \frac{4}{\Delta t_n}\{\dot{D}\}_{t_n} - \{\ddot{D}\}_{t_n} \tag{18c}$$

It should be noted that the only unknown variable in these expressions is the displacement increment $\{\Delta D\}$. Substituting the Eq. (18) into Eq. (15), the results become,

$$[\bar{K}]\{\Delta D\} = \{\Delta F^{ext}\} - \{\Delta F^{vis}\} + \{\bar{F}\} \tag{19}$$

where

$$[\bar{K}] = [K] + \frac{4}{\Delta t_n^2}[M] \tag{20}$$

$$\{\bar{F}\} = [M]\left(\{\ddot{D}\}_{t_n} + \frac{4}{\Delta t_n}\{\dot{D}\}_{t_n}\right) \tag{21}$$

Equations (18) ~ (21) are the basis of the global algorithm used in the dynamic analysis of viscoelastic solids by the LW-FEM. It is important to note that the algorithm is purely incremental, that means that no iterations are performed in the entire procedure. Another important aspect is that the effective stiffness matrix $[\bar{K}]$ will remain constant and will not have to be regenerated on each time increment Δt_n. Therefore, this matrix can be assembled and factorized only at the first time step or when the time increment Δt_n. This factorization is the most expensive part of the solution of the linear system described by Eq. (19) [36].

5. NUMERICAL ALGORITHM

Based on the above presented formulation, a computer program was developed. In the following, an outline of the step-by-step calculations performed in the code is provided, it is supposed that the field variables $\{D\}$, $\{\dot{D}\}_{t_n}$, $\{\ddot{D}\}$, $\{\varepsilon_{ij}\}$, $\{\sigma_{ij}\}$ and $S^{(m)}_{ijkl}$ are known at time t_n and a fixed value of the time increment (Δt_n) is used in all computations.

1. Firstly, the components of the relaxation tensor (*i.e.*, $\bar{C}_{ijkl}$) is computed from Eq. (4) and the global linear viscoelastic stiffness matrix $[K_{ij}]$, $[M_{ij}]$ and $[\bar{K}_{ij}]$ are evaluated from Eqs. (A.1 ~ 3) presented in the appendix A and Eq. (20),
2. $\{\Delta\sigma^R_{ij}\}$ is calculated from Eqs. (5) and (6)
3. The load vector $\{\Delta F^{vis}\}$ is obtained from Eq. (5) and Eqs. (A. 4 ~ 6), respectively,
4. The reduced load vector $\{\bar{F}\}$ is obtained from Eq. (21) and then the external load vector $\{\Delta F^{ext}\}$ is introduced into the equilibrium Eq. (19) and the nodal displacement increment vector $\{\Delta D\}$ is achieved by solving the system of equilibrium Eq. (19),
5. The strain increment components $\Delta\varepsilon_{ij}$ are computed from Eqs. 12(a) ~ 12(d),
6. The stress increments $\Delta\sigma_{ij}$ are evaluated via Eq. (3),
7. The field variables (displacements, velocities, accelerations, stress and strain tensor components) are updated at the end of the time increment Δt_n,

$$\begin{aligned}
&\{D\}_{t_{n+1}} = \{D\}_{t_n} + \{\Delta D\}_{t_n} \,,\\
&\{\dot{D}\}_{t_{n+1}} = \frac{2}{\Delta t_n}\{\Delta D\}_{t_n} - \{\dot{D}\}_{t_n} \,,\\
&\{\ddot{D}\}_{t_{n+1}} = \frac{4}{\Delta t_n^{\,2}}\{\Delta D\}_{t_n} - \frac{4}{\Delta t_n}\{\dot{D}\}_{t_n} - \{\ddot{D}\}_{t_n}\\
&\{\varepsilon_{ij}\}_{t_{n+1}} = \{\varepsilon_{ij}\}_{t_n} + \{\Delta\varepsilon_{ij}\}_{t_n} \,,\\
&\{\sigma_{ij}\}_{t_{n+1}} = \{\sigma_{ij}\}_{t_n} + \{\Delta\sigma_{ij}\}_{t_n}
\end{aligned} \tag{22}$$

8. The loop is repeated from step (1).

This numerical algorithm is also shown in Fig. 2.

6. NUMERICAL RESULTS

In this section, the convergence and numerical stability of the method against the number of elements along the radial and axial direction is verified and then the accuracy of the presented formulation and method of solution is validated. Then a multilayered pavement structure which is composed of a viscoelastic layer and three elastic layers are analyzed and numerical results are presented.

The convergence behavior of the method in analyzing a four-layered pavement with a viscoelastic layer versus the number of nodes along the radial and thickness directions is studied. A four-layered pavement composed of a viscoelastic asphalt concrete (AC) layer and elastic base, granular sub-base and sub-grade layers with parameters listed in Table 1. Also, the viscoelastic material constants of the AC layer used in the relaxation function presented in Eq. (2) are listed in Table 2.

The pavement layers are assumed to be homogeneous and isotropic. In addition, it is assumed that the layers are perfectly bonded and thus, the tractions and displacements are continuous across the interface of the adjacent layers. A time-dependent load is applied on a circular region of radius *a* on the top surface (*i.e.*, $z = 0$ plane) of the pavement, which is assumed to vary as follows [38]

https://doi.org/10.1017/jmech.2014.42 Published online by Cambridge University Press

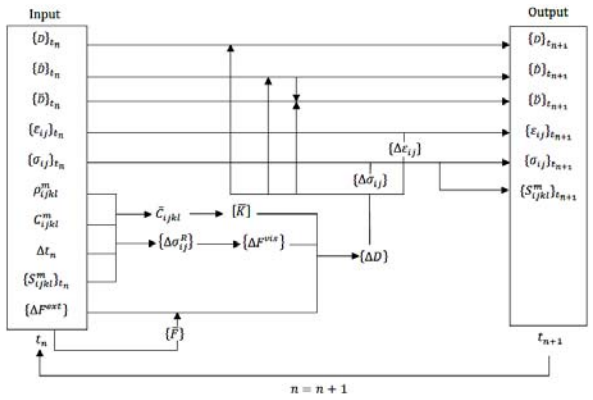


Fig. 2 Numerical algorithm.

Table 1 Material properties and thickness of layers in the four layer pavement.

Layer	Thickness (m)	Young's modulus (MPa)	Poisson's ratio	Density (kg/m^3)
AC	0.15	Viscoelastic (Table2)	0.35	2300
Base	0.2	500	0.3	2200
Subbase	0.2	200	0.3	2000
Subgrade	6.95	100	0.3	1700

Table 2 The values of C^m and ρ^m for viscoelastic AC layer [37].

m	C^m (kPa)	ρ^m (s)
0	1172	–
1	3.10×10^6	2.20×10^{-5}
2	4.31×10^6	2.20×10^{-4}
3	3.46×10^6	2.20×10^{-3}
4	2.02×10^6	2.20×10^{-2}
5	1.27×10^6	2.20×10^{-1}
6	2.72×10^5	2.20×10^{0}
7	6.59×10^4	2.20×10^{1}
8	1.45×10^4	2.20×10^{2}
9	1.52×10^3	2.20×10^{3}
10	7.10×10^2	2.20×10^{4}
11	5.88×10^1	2.20×10^{5}

$$\sigma_{zz}(r, 0) = \begin{cases} -q_0 \sin^2\left(\dfrac{\pi t}{d}\right) H(t) & r < a \\ 0 & r > a \end{cases},$$
$$q_0 = 550 \text{ (KPa)}, \quad a = 0.15 \text{ (m)} \qquad (23)$$

where q_0 is the load amplitude and d is the load duration. The computational domain has a size of $50a$ in the vertical direction and $20a$ in the horizontal direction. Also, a value of the load's duration (d) of 0.1 (s) corresponding to the vehicle speed of 10km/h is considered. The dynamic analysis of the pavement is conducted and the convergence behavior of the vertical displacement $W(0, 0, t)$ of the pavement structure at $t = 0.05$ (s) are shown in Table 3. For the comparison purpose, the same problem is analyzed using the ABAQUS software. The fast rate of convergence of the result and its excellent agreement with those of ABAQUS software is quite evident.

Finally, using the present approach, the influence of two different values of the load's duration (d) of 0.1 (s) and 0.006 (s) corresponding to the vehicle speed of 10km/h and 120km/h, respectively, on the dynamic response of the multilayered pavement are studied to evaluate the importance of the vehicle velocity effects. The number of pavement layers, material properties and loading are the same as the previous example. In Figs. 3(a) ~ 3(d), the time histories of the transverse displacement $w(0, 0, t)$ (on the top surface of the viscoelastic AC layer), the shear stress $\sigma_{rz}(0, 0.15, t)$, the radial normal stress $\sigma_{rr}(0, 0.15, t)$ and the radial strain $\varepsilon_{rr}(0, -0.15, t)$ at the bottom of the viscoelastic AC layer are presented. It is obvious that the load duration has significant effect on the variation of the transverse displacement $w(0, 0, t)$, radial stress $\sigma_{rr}(0, 0.15, t)$ and radial strain $\varepsilon_{rr}(0, 0.15, t)$ at the bottom of the viscoelastic AC layer. Also, it can be seen that as speed increases, radial strains decrease and radial stresses increase.

Through the depth variation of the transverse normal strain $\varepsilon_{zz}(0, z, t)$ and stress $\sigma_{zz}(0, z, t)$ of the pavement at $t = 0.05$ (s) and for a pulse of 0.1 (s) (vehicle speed of 10km/h) in dynamic analysis are shown in Figs. 4(a) and 4(b). It can be seen that the presented formulation and method of solution can capture the zig-zag variation of the normal strain and the smooth variation of the transverse normal stress. Also, it is obvious that as speed increases, normal strains and stress decrease. Figs. 5(a) and 5(b) show the through the depth variation of the radial strain $\varepsilon_{rr}(0, z, t)$ and stress $\sigma_{rr}(0, z, t)$ of the pavement for a pulse of 0.006 (s) (vehicle speed of 120km/h) at $t = 0.003$ (s) in dynamic analysis. It can be seen the continuous conditions at the layer interface in variation of the radial strain and discontinuity conditions at the layer interface in variation of the radial stress.

7. CONCLUSIONS

An axisymmetric layerwise finite element method to solve the time-dependent response of the multilayered viscoelastic pavement under surface loadings was presented. The LW-FE analysis was incorporated with the incremental formulation in the temporal domain for the asphalt concrete viscoelastic properties and dynamic loadings. The constitutive behavior of the viscoelastic layers was modeled using the Prony series. The formulation was based on the two-dimensional elasticity theory. The two-dimensional elasticity theory approach guarantees the generality of the method and the

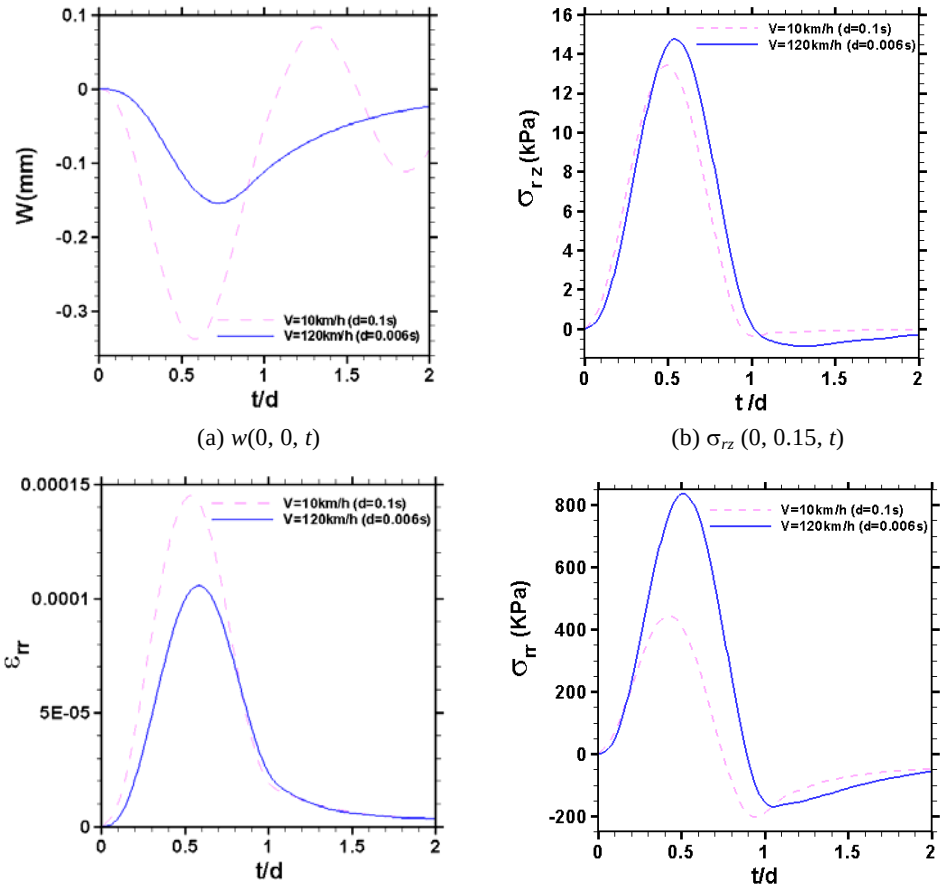
https://doi.org/10.1017/jmech.2014.42 Published online by Cambridge University Press

Table 3 The convergence and accuracy of the vertical displacement in a four layered pavement at [t = 0.05 (s)].

$N_r \times N_z$	13 × 17	21 × 27	25 × 33	29 × 39	31 × 41	33 × 43	ABAQUS[a]
$10^4 \times W(0, 0, t)$[b]	−3.398	−3.281	−3.252	−3.243	−3.241	−3.241	−3.213

[a] 1970 linear quadrilateral elements of type CAX4R

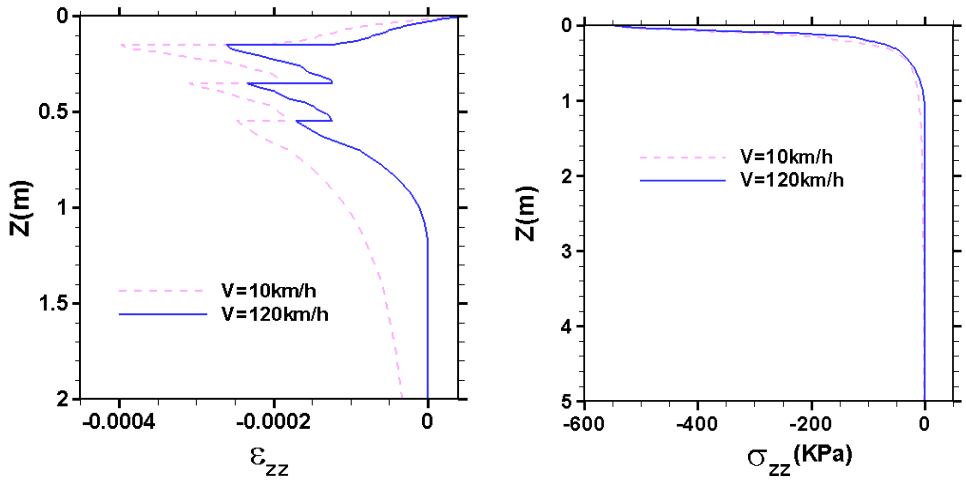
[b] $\Delta t = 0.001$



(a) $w(0, 0, t)$ (b) σ_{rz} $(0, 0.15, t)$

(c) $\varepsilon_{rr}(0, 0.15, t)$ (d) σ_{rr} $(0, 0.15, t)$

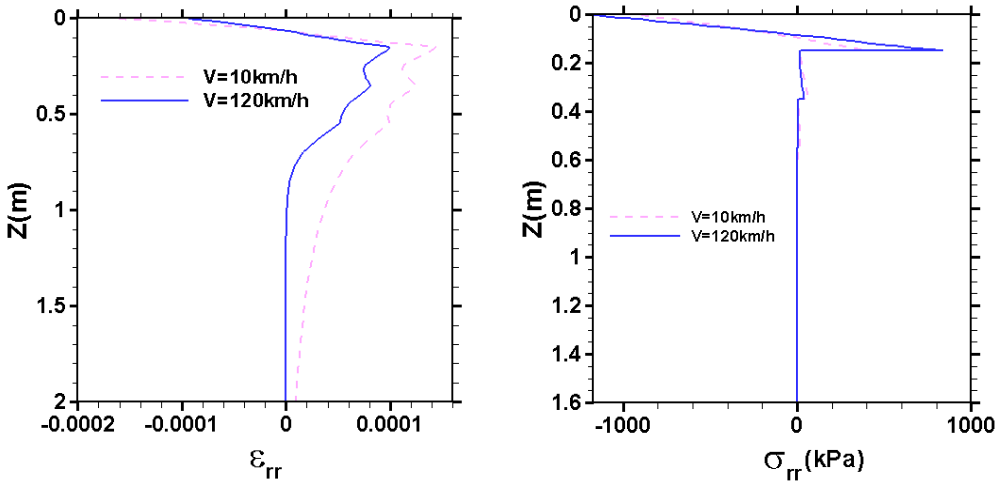
Fig. 3(a) ~ 3(d) Comparison of the time histories of the vertical displacement $w(0, 0, t)$, shear stressσ_{rz} $(0, 0.15, t)$, radial strain $\varepsilon_{rr}(0, 0.15, t)$ and radial stress σ_{rr} $(0, 0.15, t)$ of four layers pavement for two different load duration.



(a) (b)

Fig. 4(a), 4(b) The depth variations of the transverse normal strain (ε_{zz}) and stress (σ_{zz}) along the symmetry axis ($r = 0$) for two load duration of 0.1 (s) at $t = 0.05$ (s) and 0.006 (s) at $t = 0.003$ (s).

https://doi.org/10.1017/jmech.2014.42 Published online by Cambridge University Press



(a) (b)

Fig. 5(a), 5(b) The depth variations of the radial normal strain (ε_{rr}) and stress (σ_{rr}) along the symmetry axis ($r = 0$) for two load duration of 0.1 (s) at $t = 0.05$ (s) and 0.006 (s) at $t = 0.003$ (s).

layerwise theory makes the analysis economical and optimal. This method also avoids the numerical complexity in the integral transform methods in the traditional numerical handling of viscoelasticity. To validate the presented approach, the results were compared with those of the ABAQUS software. Finally, the effect of the load duration on the time histories of the transverse displacement, strain and stress components of the asphalt concrete pavements under the dynamic condition was exhibited.

APPENDIX A

The elements of the stiffness matrices $[K_{ij}]$, the mass matrices $[M_{ij}]$ in Eq. (14) are as follows, respectively,

$$[K_{uu}] = A_{p11}^{jr} D_c^{is} + A_{p13}^{jr} E_c^{is} + B_{p14}^{rj} B_c^{is} + A_{p13}^{jr} E_c^{si} + A_{p33}^{jr} H_c^{is} + B_{p34}^{rj} F_c^{is} + B_{p14}^{jr} B_c^{si} + B_{p34}^{jr} F_c^{is} + D_{p44}^{jr} A_c^{is} , \quad \text{(A.1a)}$$

$$[K_{uw}] = B_{p12}^{rj} B_c^{is} + A_{p14}^{jr} D_c^{is} + B_{p23}^{rj} F_c^{is} + A_{p34}^{jr} E_c^{si} + D_{p24}^{rj} A_c^{is} + B_{p44}^{jr} B_c^{si} , \quad \text{(A.1b)}$$

$$[K_{wu}] = B_{p12}^{jr} B_c^{si} + B_{p23}^{jr} F_c^{is} + D_{p24}^{jr} A_c^{is} + A_{p14}^{jr} D_c^{is} + A_{p34}^{rj} E_c^{is} + B_{p44}^{rj} B_c^{is} , \quad \text{(A.1c)}$$

$$[K_{ww}] = D_{p22}^{jr} A_c^{is} + B_{p24}^{jr} B_c^{si} + B_{p24}^{rj} B_c^{is} + A_{p44}^{jr} D_c^{is} \quad \text{(A.1d)}$$

$$[M_{uu}] = A_c^{is} I_p^{jr} , \quad \text{(A.2a)}$$

$$[M_{ww}] = A_c^{is} I_p^{jr} \quad \text{(A.2b)}$$

where

$$A_{pmn}^{jr} = \int_0^h \bar{C}_{pmn}(t_n) \psi_j(z) \psi_r(z)\, dz , \quad \text{(A.3a)}$$

$$B_{pmn}^{rj} = \int_0^h \bar{C}_{pmn}(t_n) \psi_j(z) \frac{d\psi_r(z)}{dz} dz , \quad \text{(A.3b)}$$

$$B_{pmn}^{jr} = \int_0^h \bar{C}_{pmn}(t_n) \psi_r(z) \frac{d\psi_j(z)}{dz} dz , \quad \text{(A.3c)}$$

$$D_{pmn}^{jr} = \int_0^h \bar{C}_{pmn}(t_n) \frac{d\psi_j(z)}{dz} \frac{d\psi_r(z)}{dz} dz , \quad \text{(A.3d)}$$

$$A_c^{is} = \int_{R_i}^{R_o} r \phi_i(r) \phi_s(r)\, dr , \quad \text{(A.3e)}$$

$$B_c^{is} = \int_{R_i}^{R_o} r \frac{d\phi_i(r)}{dr} \phi_s(r)\, dr , \quad \text{(A.3f)}$$

$$D_c^{is} = \int_{R_i}^{R_o} r \frac{d\phi_i(r)}{dr} \frac{d\phi_s(r)}{dr} dr , \quad \text{(A.3g)}$$

$$E_c^{is} = \int_{R_i}^{R_o} \frac{d\phi_i(r)}{dr} \frac{\phi_s(r)}{dr} dr , \quad \text{(A.3h)}$$

$$F_c^{is} = \int_{R_i}^{R_o} \phi_i(r) \phi_s(r)\, dr , \quad \text{(A.3i)}$$

$$H_c^{is} = \int_{R_i}^{R_o} \frac{\phi_i(r) \phi_s(r)}{r} dr , \quad \text{(A.3j)}$$

$$I_p^{jr} = \int_0^h \rho \psi_j(z) \psi_r(z) dz \quad \text{(A.3k)}$$

where $\bar{C}_{pmn}(t_n)$ is the $m \times n$ element of the viscoelastic constitutive matrix.

Also, the components of the load vector increments $\begin{Bmatrix} \{\Delta f_r\} \\ \{\Delta f_z\} \end{Bmatrix}_{t_n}$ and $\begin{Bmatrix} \{\Delta f_r^R\} \\ \{\Delta f_z^R\} \end{Bmatrix}$ in Eq. (14) are as follows, respectively,

https://doi.org/10.1017/jmech.2014.42 Published online by Cambridge University Press

$$\{\Delta f_r\} = \delta_{i1} \int_0^h \Delta q_r(z)\,\psi_j(z) r dz\,, \tag{A.4a}$$

$$\{\Delta f_z\} = \delta_{jN_z} \int_{R_i}^{R_o} \Delta q_z(r)\,\phi_i(r) r dr \tag{A.4b}$$

$$\{\Delta f_r^R\} = \tilde{E}_{rr}^i\, E_c^j + \tilde{E}_{\theta\theta}^i E_c^j + \tilde{F}_{rz}^i f_c^j\,, \tag{A.5a}$$

$$\{\Delta f_z^R\} = \tilde{E}_{zz}^i\, f_c^j + \tilde{E}_{rz}^i\, E_c^j \tag{A.5b}$$

where

$$\tilde{E}_{rr}^i = \int_{R_i}^{R_o} r \frac{d\phi_i(r)}{dr} \Delta\sigma_{rr}^R\, dr\,, \tag{A.6a}$$

$$\tilde{E}_{\theta\theta}^i = \int_{R_i}^{R_o} \phi_i(r)\,\Delta\sigma_{\theta\theta}^R\, dr\,, \tag{A.6b}$$

$$\tilde{E}_{zz}^i = \int_{R_i}^{R_o} r\phi_i(r)\,\Delta\sigma_{zz}^R\, dr\,, \tag{A.6c}$$

$$\tilde{E}_{rz}^i = \int_{R_i}^{R_o} r \frac{d\phi_i(r)}{dr} \Delta\sigma_{rz}^R\, dr\,, \tag{A.6d}$$

$$\tilde{F}_{rz}^i = \int_{R_i}^{R_o} r\phi_i(r) \Delta\sigma_{rz}^R\, dr\,, \tag{A.6e}$$

$$E_c^j = \int_0^h \psi_j(z)\, dz\,, \tag{A.6f}$$

$$f_c^j = \int_0^h \frac{d\psi_j(z)}{dz}\, dz = \psi_j(0) - \psi_j(-h)\,, \tag{A.6g}$$

$$f_c^i = \int_{R_i}^{R_o} \phi_i(r)\, dr \tag{A.6h}$$

ACKNOWLEDGEMENTS

The first and third authors acknowledge the financial support received from the Persian Gulf University.

REFERENCES

1. Jianlin, W. and Bjorn, B., "A Time Domain Boundary Element Method for Modeling the Quasi-Static Viscoelastic Behavior of Asphalt Pavements," *Engineering Analysis with Boundary Elements*, **31**, pp. 226–240 (2007).
2. Al-Huniti, N., Al-Faqs, F. and Abu Zaid, O., "Finite Element Dynamic Analysis of Laminated Viscoelastic Structures," *Applied Composite Materials*, **17**, pp. 489–498 (2010).
3. Jaeseung, K., "General Viscoelastic Solutions for Multilayered Systems Subjected to Static and Moving Loads," *Journal of Materials in Civil Engineering*, **23**, pp. 1007–1016 (2011).
4. Chen, E. Y. G., Pan, E., Norfolk, T. S. and Wang, Q., "Surface Loading of a Multilayered Viscoelastic Pavement: Moving Dynamic Load," *Road Materials and Pavement Design*, **12**, pp. 849–874 (2011).
5. Ameri, M., Malakouti, M. and Malekzadeh, P., "Quasi-Static Analysis of Multilayered Domains with Viscoelastic Layer Using Incremental-Layerwise Finite Element Method," *Mechanics of Time-Dependent Materials*, **18**, pp. 275–291 (2014).
6. Bozza, A. and Gentili, G., "Inversion and Quasi-Static Problems in Linear Viscoelasticity," *Meccanica*, **30**, pp. 321–335 (1995).
7. Drozdov, A. D. and Dorfmann, A., "A Constitutive Model in Finite Viscoelasticity of Particle-Reinforced Rubbers," *Meccanica*, **39**, pp. 245–270 (2004).
8. Ghazlan, G., Caperaa S. and Petit, C., "An Incremental Formulation for the Linear Analysis of Thin Viscoelastic Structures Using Generalized Variables," *International Journal for Numerical Methods in Engineering*, **38**, pp. 3315–3333 (1995).
9. Zocher, M. A., Groves, S. E. and Aellen, D. H., "A Three-Dimensional Finite Element Formulation for Thermoviscoelastic Orthotropic Media," *International Journal for Numerical Methods in Engineering*, **40**, pp. 2267–2288 (1997).
10. Kim, K. S. and Sung Lee, H., "An Incremental Formulation for the Prediction of Two-Dimensional Fatigue Crack Growth with Curved Paths," *International Journal for Numerical Methods in Engineering*, **72**, pp. 697–721 (2007).
11. Theocaris, P. S., "Creep and Relaxation Contraction Ratio of Linear Viscoelastic Materials," *Journal of the Mechanics and Physics of Solids*, **12**, pp. 125–138 (1964).
12. Chazal, C. and Pitti, R. M., "An Incremental Constitutive Law for Ageing Viscoelastic Materials, a Three Dimensional Approach," *Comptes Rendus Mecanique*, **337**, pp. 30–33 (2009).
13. Dubois, F., Chazal, C. and Petit, C., "A Finite Element Analysis of Creep-Crack Growth in Viscoelastic Media," *Mechanics of Time-Dependent Materials*, **2**, pp. 269–286 (1999).
14. Chen, W. H. and Lin, T. C., "Dynamic Analysis of Viscoelastic Structures Using Incremental Finite Element Method," *Engineering Structures*, **4**, pp. 271–276 (1982).
15. Chen, E., Pan, E. and Green, R., "Surface Loading of a Multilayered Viscoelastic Pavement: Semi Analytical Solution," *Journal of Engineering Mechanics*, **35**, pp. 517–528 (2009).
16. Gibson, N. H., Schwartz, C. W., Schapery, R. A. and Witczak, M. W., "Viscoelastic, Viscoplastic, and Damage Modeling of Asphalt Concrete in Unconfined Compression," *Transport Research Record*, **1860**, pp. 3–15 (2003).
17. Elseifi, M. A., Al-Qadi, I. L. and Yoo, P. J., "Viscoelastic Modeling and Field Validation of Flexible Pavement," *Journal of Engineering Mechanics*, **132**, pp. 172–178 (2006).
18. Ghoreishy, M. H. R., "Determination of the Parameters of the Prony Series in Hyper-Viscoelastic Material Models Using the Finite Element Method," *Materials and Design*, **35**, pp. 791–797 (2012).
19. Mulungye, R. M., Owende, P. M. O. and Mellon, K., "Finite Element Modelling of Flexible Pavements on

https://doi.org/10.1017/jmech.2014.42 Published online by Cambridge University Press

Soft Soil Subgrades," *Materials and Design*, **28**, pp. 739–756 (2007).
20. Pellinen, T. K. and Witczak, M. W., "Use of Stiffness of Hot-Mix Asphalt as a Simple Performance Test," *Transport Research Record*, **1789**, pp. 80–90 (2002).
21. Olard, F., Benedetto, H. D., Dony, A. and Vaniscote, J. C., "Properties of Bituminous Mixtures at Low Temperatures and Relations with Binder Characteristics," *Material and Structure*, **38**, pp. 121–126 (2005).
22. Chupin, O., Chabot, A., Piau, J. M. and Duhamel, D., "Influence of Sliding Interfaces on the Response of a Layered Viscoelastic Medium Under a Moving Load," *International Journal of Solids and Structures*, **47**, pp. 3435–3446 (2010).
23. Bahia, H. U. and Anderson, D. A., "The Development of the Bending Beam Rheometer, Basics and Critical Evaluation of the Rheometer," *ASTM Physical Properties of Asphalt Cement Binders Conference*, **1241**, pp. 28–50 (1995).
24. Reddy, J. N., "A Generalization of Two-Dimensional Theories of Laminated Composite Plates," *Communications in Applied Numerical Methods*, **3**, pp. 173–180 (1987).
25. Tahani, M. and Nosier, A., "Accurate Determination of Interlaminar Stresses in General Cross-Ply Laminates," *Mechanics of Advanced Materials and Structures*, **11**, pp. 67–92 (2004).
26. Malekzadeh, P., Setoodeh, A. R. and Barmshouri, E., "A Hybrid Layerwise and Differential Quadrature Method for In-Plane Free Vibration of Laminated Thick Circular Arches," *Journal of Sound and Vibration*, **315**, pp. 212–225 (2008).
27. Shakeri, M. and Mirzaeifar, R., "Static and Dynamic Analysis of Thick Functionally Graded Plates with Piezoelectric Layers Using Layerwise Finite Element Model," *Mechanics of Advanced Materials and Structures*, **16**, pp. 561–575 (2009).
28. Setoodeh, A. R., Malekzadeh, P. and Nikbin, K., "Low Velocity Impact Analysis of Laminated Composite Plates Using a 3D Elasticity Based Layerwise FEM," *Materials and Design*, **30**, pp. 3795–3801 (2009).
29. Setoodeh, A. R. and Karami G., "Static Free Vibration and Buckling Analysis of Anisotropic Thick Laminated Composite Plates on Distributed and Point Elastic Supports Using a 3-D Layer-Wise FEM," *Journal of Engineering Structures*, **26**, pp. 211–220 (2004).
30. Tahani, M., "Analysis of Laminated Composite Beams Using Layerwise Displacement Theories," *Composite Structure*, **79**, pp. 535–547 (2007).
31. Malekzadeh, P., "A Two-Dimensional Layerwise-Differential Quadrature Static Analysis of Thick Laminated Composite Circular Arches," *Applied Mathematical Modelling*, **33**, pp. 1850–1861 (2009).
32. Boltzmann, L., "Zur Theorie Der Elastischen Nachwirkung Sitzungsber," *Mat Naturwiss Kl Kaiser Akad Wiss*, pp. 70–275 (1878).
33. Picoux, B., ElAyadi, A. and Petit, C., "Dynamic Response of a Flexible Pavement Submitted by Impulsive Loading," *Soil Dynamics and Earthquake Engineering*, **29**, pp. 845–854 (2009).
34. Dave Eshan, V., Paulino Glaucio, H. and Buttlar William, G., "Viscoelastic Functionally Graded Finite-Element Method Using Correspondence Principle," *Journal of Materials in Civil Engineering*, **23**, pp. 39–48 (2011).
35. Kim, J., Roque, R. and Byron, T., "Viscoelastic Analysis of Flexible Pavements and Its Effects on Top-Down Cracking," *Journal of Materials in Civil Engineering*, **21**, pp. 324–332 (2009).
36. Bathe, K. J., *Finite Element Procedures*, 2rd Edition, New Jersey: Prentice-Hall (1996).
37. Lee, H. J., "Uniaxial Constitutive Modeling of Asphalt Concrete Using Viscoelasticity and Continuum Damage Theory," PhD Dissertation, North Carolina State University, Raleigh, NC (1996).
38. Huang, Y. H., *Pavement Analysis and Design*, 2rd Edition, Pearson Prentice Hall, Upper Saddle River, NJ (2004).

(Manuscript received August 6, 2013,
accepted for publication February 14, 2014.)

https://doi.org/10.1017/jmech.2014.42 Published online by Cambridge University Press